Stress Defocusing in Anisotropic Compaction of Thin Sheets

B. Roman*
PMMH, UMR 7636 ESPCI/CNRS/Paris 6/Paris 7, 10 rue Vauquelin, 75231 Paris CEDEX 05, France

A. Pocheau†
Aix-Marseille Université, IRPHE, 13384, Marseille, France; CNRS, IRPHE, 13384, Marseille, France
(Received 30 May 2011; revised manuscript received 16 November 2011; published 15 February 2012)

We address the crumpling of thin sheets in between large scale curved cylinders. In contrast with the usual crushing of a paper ball, one curvature of the sheet is fixed here by the cylinders radius, yielding an anisotropic compaction. As compaction proceeds, it is found that sheets first develop singular folds involving ridges or developable cones, but eventually turn to regular folds free of any geometrical singularities, without ever having entered the plastic regime. This surprising uncrumpling transition corresponds to a stress defocusing. It is understood from a balance between bending and stretching energies on regular states.

DOI: 10.1103/PhysRevLett.108.074301 PACS numbers: 46.32.+x, 46.70.−p, 62.20.−x

It is our common experience that thin sheets crumple when not manipulated with care; sharp ridges and singular points then appear and focus the deformation [1], often yielding irreversible scars when exceeding the plastic limit. The same remains true at the microfabrication scale [2], and even for atom thick sheets of graphene, with important implications for their electronic properties [3].

Why do thin sheets crumple? Consider a thin sheet of typical size L fitted into a shrinking spherical volume [4–6] with radius $R \ll L$. This compaction may be called isotropic since it involves a similar reduction of all dimensions, as in the crushing of a ball of paper. Let us first consider a solution with no singularities, so that all length scales (e.g., principal radius of curvature, out-of plane displacement) would be proportional to the radius R of the sphere. Such a surface involves nonzero Gaussian curvature and therefore in-plane stretching because of the Gauss' *theorema egregium* which states that surfaces could not change their Gaussian curvature without changing distances. In this case the strains will be of order 1, as when a disk is forced to take the shape of a hemisphere [7]. The bending and stretching energies would then, respectively, read $E_b \sim Eh^3R^{-2}S$, $E_s \sim EhS$, S denoting the sheet area [8]. As $E_s/E_b \sim (R/h)^2$ is large for a thin sheet ($h \ll R$), stretching completely dominates the energy balance. It is then reasonable to imagine that the minimum energy state will be of a different type, close to piecewise isometric surfaces that are free of stretching. However, singularities will be usually required to match the isometric pieces [9]: the sheet crumples. The size of the core of these crumpling singularities (ridges [8,10–12] or d-cones [8,9,13–15]) depends on thickness h and their number increases with compaction.

However, the above isotropic compaction is particular in the sense that it enforces similar curvatures in all directions. We show in this Letter that it thus misses some interesting features displayed on compaction routes involving significantly different principal curvatures. In particular, the sheet may then undergo a spontaneous reverse uncrumpling at large anisotropic compaction.

In the experiment, a thin polycarbonate planar sheet (length $l = 155$ mm, width $L = 190$ mm, thickness h ranging from 0.05 to 0.5 mm) is clamped along its largest side l onto the arches of a transparent upper cylinder whose curvature radius $R = 50$ cm is large (Fig. 1). As the distance between the clamping arches, $X = 180$ mm, is smaller than the sheet width L, the sheet is already buckled before compression (Fig. 2). A bottom cylinder, parallel to the upper one, is then moved up so as to impose a gap Y between them. Further evolution of the gap Y is then set and controlled by stepper motors to an accuracy of a tenth of microns [16,17], thus allowing a detailed study of the compaction. Whereas one of the principal curvature of the sheet c_1 is induced by iterated buckling, a second one c_2 is imposed by the cylinders curvature (Fig. 1). Both yield a

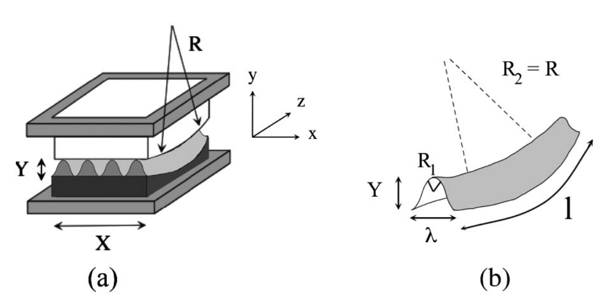

FIG. 1. A compressing device (a) involves cylindrical plates distant from a controlled gap Y and a sheet clamped on their curved sides in between. (b) By iterative buckling, gap reduction yields the generation of folds of ever smaller size λ, whose axis is bent by the cylinders. This results in two principal curvatures and thus in Gaussian curvature and in-plane stretching.

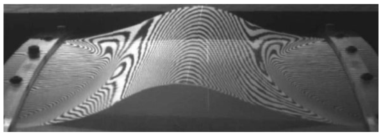

FIG. 2. Clamped sheet prior compression showing two ridges at the contact lines between the sheet and the cylinder.

nonzero Gaussian curvature $G = c_1c_2$ and stretching, in any states.

In view of the large curvature radius ($R \gg Y$), it is instructive to consider the specific case of compaction between parallel plates [16–18], i.e., $R = \infty$. An isometric solution with the sheet shape invariant along the clamping direction is then allowed. When reducing the gap Y, it gives rise, by iterated buckling, to successive generations of regular and identical folds. In particular, a n-fold solution can be formally constructed by repeating n times a single fold of height Y but scaled down by a factor $1/n$. It is then made of n folds of reduced height Y/n and width $\lambda = X/n$, meaning that $n \sim Y^{-1} \sim \lambda^{-1}$. In comparison, using a large but finite R here means weakly bending the axes of these folds [Fig. 1(b)]. However, as $R \gg Y$, the above geometric scaling laws are expected to hold, at least on smooth uncrumpled states.

As the gap Y is reduced, buckling makes the sheet actually display an increasing number $n \sim Y^{-1}$ of folds whose right and left sides appear, respectively, in red or blue in Fig. 3. Folds first involve a contact surface with the cylindrical plates ending by curved ridges [Figs. 3(a) and 3(b)], similar to those found in the uncompressed state of Fig. 2. These ridges condense the sheet's stretching on a curved line, similarly to a buckled ping-pong ball [19,20]. Then, on further compression, folds generate defects corresponding to d-cones [Figs. 3(c)–3(e)]. Their number grows with compression as in usual compaction but, surprisingly, below a critical gap, they all suddenly disappear before any plastic deformation could occur [Fig. 3(f)]. The sheet then simply displays line contacts with the cylindrical plates with no defect, neither ridges nor d-cones: it has selected a regular, uncrumpled state. We emphasize that stretching is, nevertheless, still present since the Gaussian curvature is not zero, but that it is no longer condensed in narrow domains. We also note that singularities actually disappeared in the bulk and not from the sides as observed on a punctually loaded arch [8]. This means that the transition to a regular state is not monitored by finite size effects here, but by an actual balance between some bulk properties. It may thus be viewed as a phase transition during which stretching evolves from a condensed state to a dilute state and whose reversibility is ensured by the absence of plastic deformation, even at the core of singularities.

As presented above, the appearance of crumpling can be predicted by studying the regular states compatible with the compaction boundaries and it is to be questioned

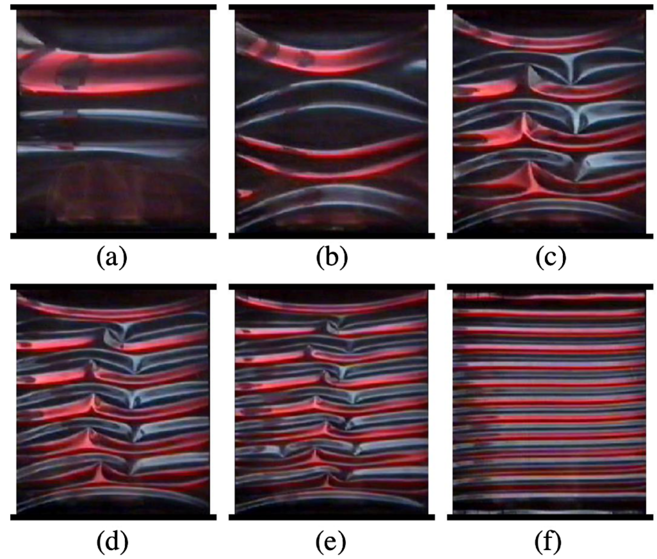

FIG. 3 (color online). Experimental pictures taken from above; $h = 180\ \mu$m. Colors refer to left (red, bright) or right (blue, bright) fold sides. Clamped sides are shown by black ticks. Compression increases from (a) to (f). (a) Single fold with ridge. (b) Two folds with ridges. (c),(d),(e) Four, six, and eight folds with ridges and d-cones. (f) Regular state of twelve folds involving no singularity. See Supplemental Material [21] for a movie of the sheet compression from (a) to (f).

whether they correspond to energy minima. Here, the bending energy density reads [20,22] $e_b = 2BC^2$ where $B = Eh^3/12(1-\nu^2)$ denotes the bending stiffness, h the sheet thickness, E the Young modulus of the material, ν its Poisson's ratio, and $C = (c_1 + c_2)/2$ the mean curvature. The in-plane stresses $\sigma_{i,j} = (-1)^{\delta_{ij}+1}\partial^2\chi/\partial_i\partial_j$, i, $j = x$, z, induced by the nonvanishing Gauss curvature $G = c_1c_2$ derive from the Airy's stress function χ which obeys the geometric Föppl–von Kármán's equation [20,22],

$$\Delta^2\chi + EG = 0, \tag{1}$$

where Δ denotes the Laplacian operator. In terms of scaling, the spatial derivatives extract the typical length scale for the variations of the sheet height and emphasize the smallest one, Λ, so that $\partial^2\chi/\partial_i\partial_j \sim \Lambda^{-2}\chi$, i, $j = x$, z. This yields $\sigma \sim \Lambda^{-2}\chi$ for in-plane stresses, $\Lambda^{-4}\chi \sim EG$ from (1) and finally, $\sigma \sim \Lambda^2 EG$. The stretching energy density then scales like $e_s \sim h\sigma^2/E \sim Eh\Lambda^4G^2$, so that the energy density ratio writes $e_s/e_b \sim \gamma^4$ with

$$\gamma = \Lambda(G/hC)^{1/2}. \tag{2}$$

This scaling estimate on regular states applies to all situations of compaction, isotropic or anisotropic. In line with the analysis of isotropic compression, one expects singular states for $\gamma \gg 1$, regular states for $\gamma \lesssim 1$ and a transition between them for γ of order 1.

Interestingly, in the present compaction by cylinders (Fig. 1), the energy densities of the smooth state can also be derived exactly, assuming invariance along the cylinder orthoradial direction z of both the sheet shape ξ_0 and the sheet stresses $(\sigma_{i,j})$. Taking into account the cylinder shape $y = z^2/2R$, the sheet surface thus writes $\xi(x, z) = \xi_0(x) + z^2/2R$, where ξ_0 is a λ-periodic function with zero mean value, λ denoting the fold width. Its principal curvatures are then close to $c_1 = \xi_0''(x)$, $c_2 = 1/R$, so that $G = \xi_0''(x)/R$. Invariance on the z axis, however, implies a stress σ_{zz} only dependent on x and constant σ_{xx} and σ_{xz} with, by symmetry, $\sigma_{xz} = 0$. Equation (1) then reduces to $d^2\sigma_{zz}/dx^2 = -E\xi_0''(x)/R$ and, finally, to $\sigma_{zz} = -E\xi_0(x)/R$. Taking $\xi_0 \approx Y/2\sin(2\pi x/\lambda)$ and noticing that the dominant stress is σ_{zz} [23], the mean energy densities on the sheet write $\bar{e}_s = Eh(Y/R)^2/16$ and $\bar{e}_b = B\pi^4Y^2/\lambda^4$, so that $\bar{e}_s/\bar{e}_b \sim 3\lambda^4/4\pi^4h^2R^2$. Using $\Lambda = \lambda/2\pi$, $c_2 = 1/R \ll Y/\Lambda^2 \sim c_1$, $C \sim c_1/2$, $G = c_1c_2$, and thus, following (2), $\gamma = (\lambda/2\pi)(2/hR)^{1/2}$, one gets $\bar{e}_s/\bar{e}_b = 3\gamma^4$, in agreement with the general estimate. We then note that mean stretching and bending energies are found equal when $\gamma = \gamma_c \sim 0.76$.

At the beginning of compression, $n = 1$ and $\lambda = X$, so that $\gamma \sim 8$ for $h = 0.05$ mm. In turn, the mean energy ratio $\bar{e}_s/\bar{e}_b = 3\gamma^4$ is dramatically large, more than 10^4 here, meaning that stretching would largely dominate bending on regular states. A singular solution, involving stretching condensed in narrow regions, should thus be energetically far more favorable. This is attested in experiment by a spontaneous sheet crumpling [Fig. 3(c)].

As the gap Y is reduced, the number n of folds grows and their size $\lambda = X/n$ decreases together with γ. Then, for $\lambda \approx 2\pi(hR/2)^{1/2}$, i.e., $\gamma \approx 1$, bending and stretching energies get about the same order of magnitude on regular states. Stretching energy is therefore not dominant and focusing stretching in narrow but highly stressed regions would no longer make the sheet elastic energy decrease. The regular state then stands as an energetically efficient solution: the sheet uncrumples [Fig. 3(f)].

The uncrumpling transition is thus expected for a critical value of the energy ratio of order unity, corresponding here to a fold number $n_c = (hR/2X^2)^{-1/2}/2\pi\gamma_c$ with $\gamma_c \sim 1$. Figure 4 shows a fair agreement with this scaling law for sheets with thicknesses varying over a decade and for a value of γ_c, 0.55, very close to the value 0.76 at which $\bar{e}_s = \bar{e}_b$. Note that this transition holds for out-of-plane deformation Y, wavelength λ, and mean curvature radius C^{-1} still much larger than the thickness h: $Y/h > 12$, $\lambda/h > 200$ and $C^{-1}/h > 50$ here.

Interestingly, the same kind of argument would also predict stress defocusing for large isotropic compaction. Indeed, on a putative regular solution, all length scales would be similar due to statistical isotropy and homogeneity, so that $\Lambda \sim G^{-1/2} \sim C^{-1}$ and $\gamma \sim (hC)^{-1/2}$. Increasing compaction and thus C, γ should thus decrease up to a value of order unity, yielding a transition to regular states: a paper ball should uncrumple when compressed

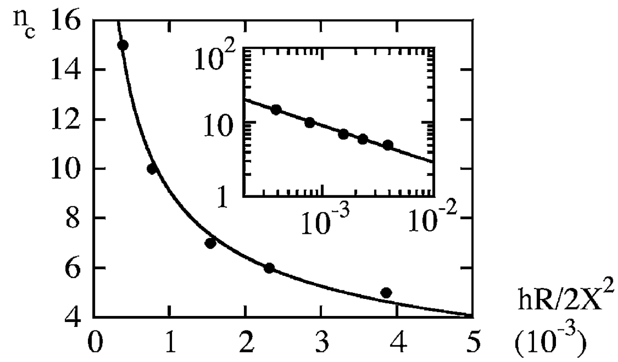

FIG. 4. Critical number of folds n_c at the uncrumpling transition for different sheet thicknesses h. Continuous line corresponds to $2\pi\gamma_c n_c = (hR/2X^2)^{-1/2}$ with $\gamma_c = 0.55$ as best fitting coefficient. Inset: same data in log-log scales.

enough. This is actually not observed in practice, because the transition condition $\gamma \sim 1$ implies extremely large curvatures $C \sim 1/h$ at which new considerations emerge. First the sheet can no longer be considered as thin, so that the separation into bending and stretching energies becomes meaningless. Second, and more importantly in practice, very large strains are in order, yielding plastic deformations. Plastic transition actually preempts the uncrumpling transition.

These arguments stress that the transition criterion $\gamma_c \sim 1$ only makes sense provided the sheet remains thin and within the elastic regime. Accordingly, the typical strains due to bending, $\epsilon_C = hC$, and stretch, $\epsilon_G = \Lambda^2G$, must remain smaller than a typical yield strain ϵ_Y for the material considered, of the order of a few percent here [24].

Our results together with the above limitations are best illustrated in a log-log phase diagram (Fig. 5) based on the adimensional parameters ϵ_G and ϵ_C. The plastic limit, beyond which considering an elastic regular state looses sense are displayed by the lines $\epsilon_G = \epsilon_Y$ and $\epsilon_C = \epsilon_Y$ with $\epsilon_Y = 5\%$ here. The isotropic compaction route $\Lambda G^{1/2} \sim 1$ corresponds to $\epsilon_G \sim 1 \gg \epsilon_Y$ and thus to a horizontal line that stands well within the plastic domain. In contrast, the anisotropic configuration studied here is characterized by $C \sim c_1 \sim Y/\Lambda^2$, $G \sim c_1c_2 \sim Y/R\Lambda^2$, and $\Lambda \sim Y$ which altogether yield $\epsilon_G \sim (h/R)\epsilon_C^{-1}$, i.e., a line with a slope -1 and a position parametrized by h/R. Noticing that $e_s/e_b = 3(\epsilon_G/\epsilon_C)^2$, the transition $e_s/e_b \sim 1$ may finally be located on the line $\epsilon_G \sim \epsilon_C/\sqrt{3}$. As evidenced experimentally, the anisotropic compaction route then actually succeeds in defocusing the elastic stretch at large compaction *before* encountering the plastic transition.

The difference between isotropic and nonisotropic compaction routes may be reinterpreted in terms of wrinkling scales and curvatures. For isotropic compaction, $\epsilon_G \sim 1$, the uncrumpling transition $\epsilon_G \sim \epsilon_C$ takes place for $\epsilon_C = hC \sim 1$ and thus for a fold scale $\lambda \sim C^{-1}$ of order h. In contrast, for the present anisotropic compaction, $\epsilon_G \sim (h/R)\epsilon_C^{-1}$, the uncrumpling transition $\epsilon_G \sim \epsilon_C$ occurs for

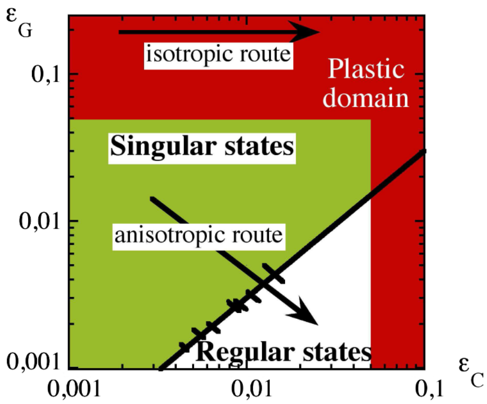

FIG. 5 (color online). Transition diagram in the variable space (ϵ_G, ϵ_C), where $\epsilon_G = hC$ and $\epsilon_C = \Lambda^2 G$ are the typical strains due to curvature, and to in-plane stretching. The isotropic route always lies in the plastic domain. In contrast, anisotropic crumpling yields elastic regularization and stress defocusing before experiencing plastic deformation. The thick line corresponds to the uncrumpling transition for $\gamma_c = 0.55$ and black ticks to the observed uncrumpling transition for h varying from 50 to 500 μm, including error bars. Note that the diagram would be similar in variables $(G/C^2, hC)$.

$\epsilon_C \sim (h/R)^{1/2}$, i.e., for a fold scale $\lambda \sim C^{-1}$ of the order of $(hR)^{1/2}$. The specificity of this route is thus to involve a new, fixed length scale, the radius of curvature $R \gg h$, following which the fold scale λ has to be compared to $(hR)^{1/2}$ instead of h to decide of the transition. As $(hR)^{1/2}$ is 30 to 100 times larger than h here, stress defocusing then succeeds to take place before plasticity here, i.e., still for $h \ll C^{-1}$, and, in particular, still in the thin sheet regime. Alternatively, the fact that λ is always of order C^{-1} whatever the kind of compaction, yields $\epsilon_G \sim G/C^2$. Accordingly, the analysis in terms of strains (ϵ_G, ϵ_C) may be reinterpreted in terms of nondimensional curvatures $(G/C^2, hC)$, emphasizing the geometrical nature of stress focusing and defocusing.

It is worth noticing that the ratio of energy densities varies as a large power of the typical fold size λ, $e_s/e_b \propto \lambda^4$, or equivalently, of the number of folds $n \approx X/\lambda$: $e_s/e_b \propto n^{-4}$. This makes it highly sensitive to the fold number, a fact which corroborates the sharpness of the transition and which relativizes the role of the scaling laws prefactors in the transition criterion.

Compressing a thin sheet in between curved plates has thus provided evidence that elastic singularities are not always the ultimate fate of crushing. In particular, all the singularities that formed at the earlier stage of compression surprisingly disappeared here on the compression route prior any plastic deformation, leaving a regular state free of any geometrical singularity. This ''uncrumpling'' transition is at variance with our usual experience of crumpled paper, where the density of singularities increases with compaction until yielding plastic deformations. Actually, in any configuration, as stretching energy always becomes less dominant over bending energy as compaction increases, there will eventually be no reason to crumple, so that an uncrumpling transition should be expected. On isotropic compaction, this transition cannot take place because curvature radii comparable to thickness are required. However, we showed here that it can indeed be observed if compaction is anisotropic.

*benoit.roman@espci.fr
†alain.pocheau@irphe.univ-mrs.fr

[1] T. A. Witten, Rev. Mod. Phys. **79**, 643 (2007).
[2] J. Genzer and J. Groenewold, Soft Matter **2**, 310 (2006).
[3] V. M. Pereira, A. H. Castro Neto, H. Y. Liang, and L. Mahadevan, Phys. Rev. Lett. **105**, 156603 (2010).
[4] H. Aharoni and E. Sharon, Nature Mater. **9**, 993 (2010).
[5] Y. C. Lin, Y. L. Wang, Y. Liu, and T. M. Hong, Phys. Rev. Lett. **101**, 125504 (2008).
[6] K. Matan, R. B. Williams, T. A. Witten, and S. R. Nagel, Phys. Rev. Lett. **88**, 076101 (2002).
[7] J. Hure, B. Roman, and J. Bico, Phys. Rev. Lett. **106**, 174301 (2011).
[8] A. Boudaoud, P. Patricio, Y. Couder, and M. Ben Amar, Nature (London) **407**, 718 (2000).
[9] M. Ben Amar and Y. Pomeau, Proc. R. Soc. A **453**, 729 (1997).
[10] A. E. Lobkovsky, S. Gentges, H. Li, D. Morse, and T. Witten, Science **270**, 1482 (1995).
[11] A. E. Lobkovsky, Phys. Rev. E **53**, 3750 (1996).
[12] A. E. Lobkovsky and T. A. Witten, Phys. Rev. E **55**, 1577 (1997).
[13] S. Chaïeb, F. Melo, and J.-C. Géminard, Phys. Rev. Lett. **80**, 2354 (1998).
[14] E. Cerda and L. Mahadevan, Phys. Rev. Lett. **80**, 2358 (1998).
[15] E. Cerda, S. Chaïeb, F. Melo, and L. Mahadevan, Nature (London) **401**, 46 (1999).
[16] B. Roman and A. Pocheau, Europhys. Lett. **46**, 602 (1999).
[17] B. Roman and A. Pocheau, J. Mech. Phys. Solids **50**, 2379 (2002).
[18] H. Chai, J. Mech. Phys. Solids **46**, 1155 (1998).
[19] A. Pogorelov, *Bendings of Surfaces and Stability of Shells* (American Mathematical Society, Providence, 1988).
[20] B. Audoly and Y. Pomeau, *Elasticity and Geometry: From Hair Curls to the Non-Linear Response of Shells* (Oxford University Press, Oxford, 2010).
[21] See Supplemental Material at http://link.aps.org/supplemental/10.1103/PhysRevLett.108.074301 for a movie of the sheet compression from Figs. 3(a) to 3(f).
[22] L. Landau and E. Lifshitz, *Theory of Elasticity* (Elsevier, New York, 1986).
[23] The force Föppl–von Kármán equation $B\Delta^2\xi - h[\chi, \xi] = 0$ yields $\sigma_{xx} \sim Eh^2/\lambda^2$, whereas geometry imposes $\lambda \sim Y$. This yields $\sigma_{zz} \sim EY/R \sim \lambda/R$ and finally $\sigma_{zz}/\sigma_{xx} \sim (\lambda^3/h^2R) > 10^{3/2}$ here.
[24] B. Du, O. C. Tsui, Q. Zhang, and T. He, Langmuir **17**, 3286 (2001).